Advanced experimental methods in nanoscale Physics

Physics of semiconductor devices

Claudia Ojeda-Aristizabal

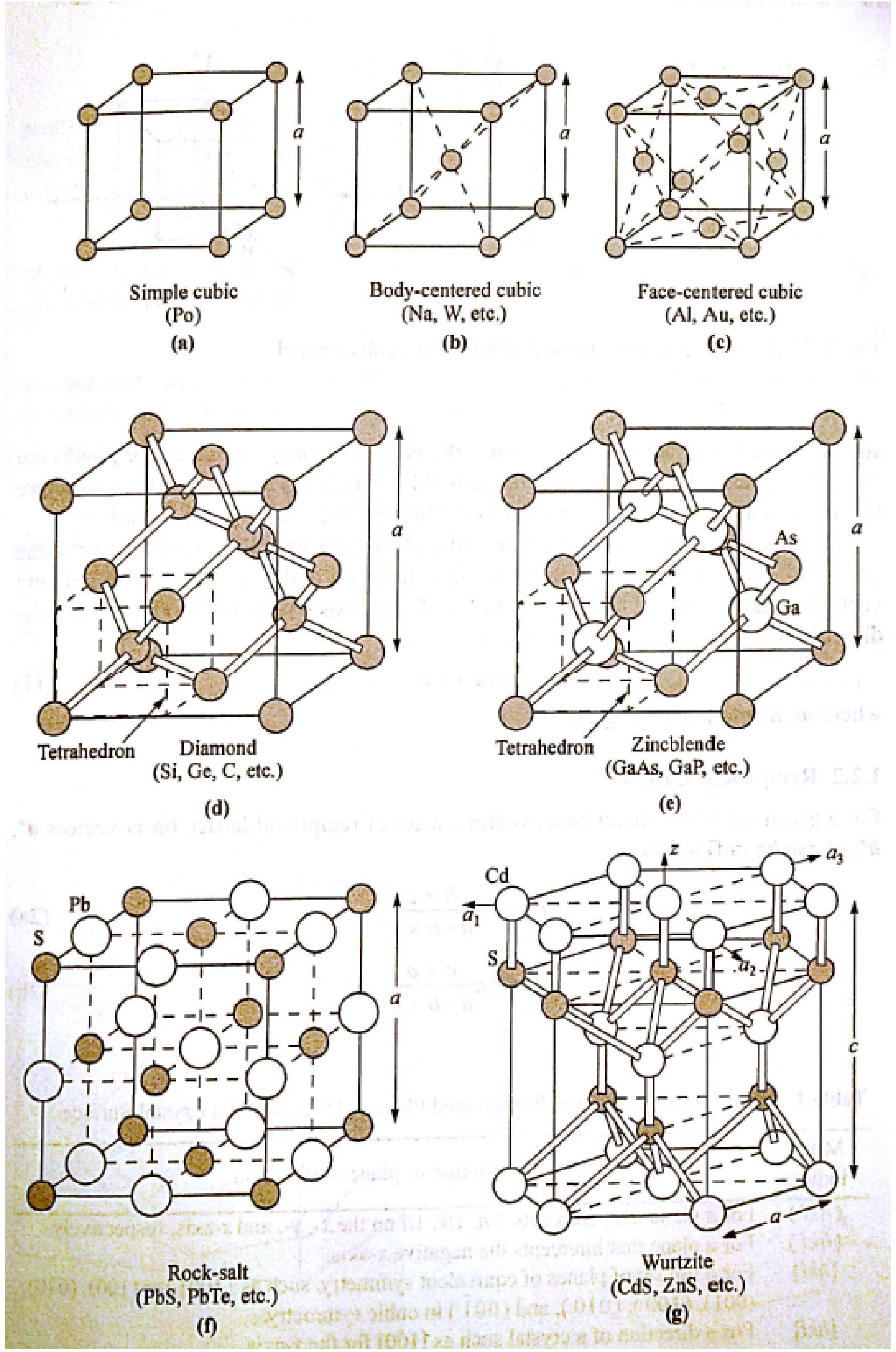

Diamond structure (silicon)

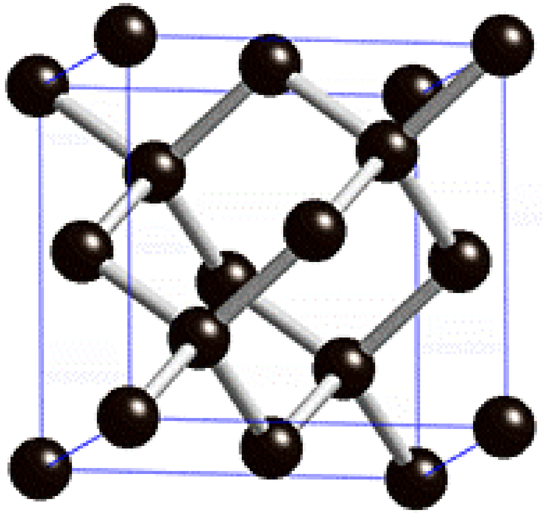

By original uploader: Brian0918 - http://www.msm.cam.ac.uk/phase-trans/2003/MP1.crystals/MP1.crystals.html ; English Wikipedia, CC0, https://commons.wikimedia.org/w/index.php?curid=349927

Miller indices

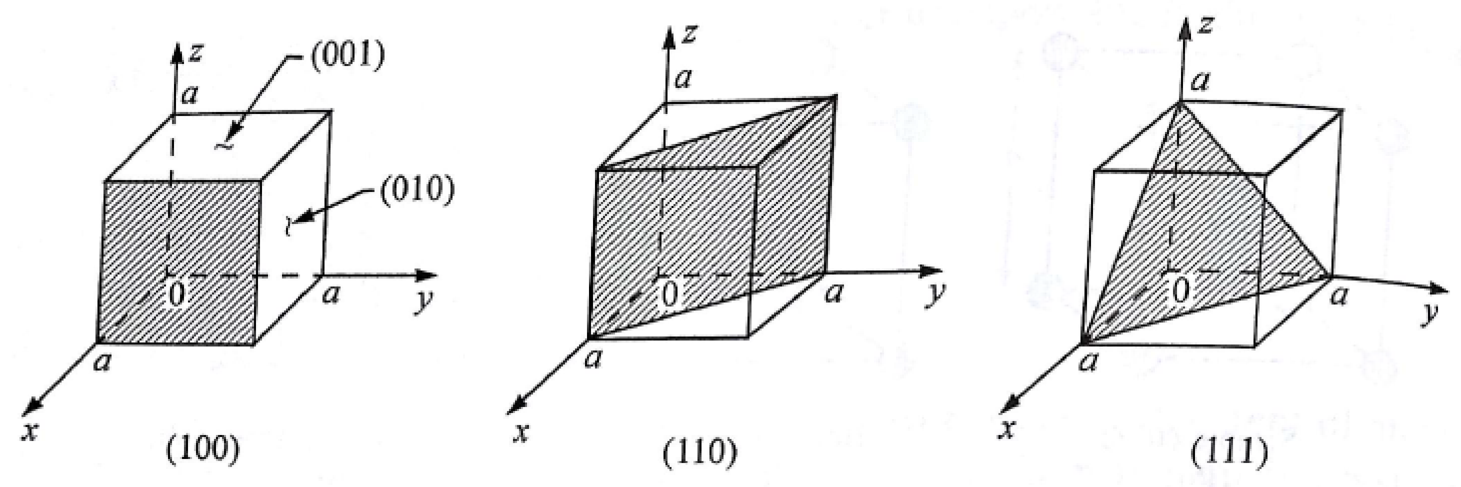

Miller indices

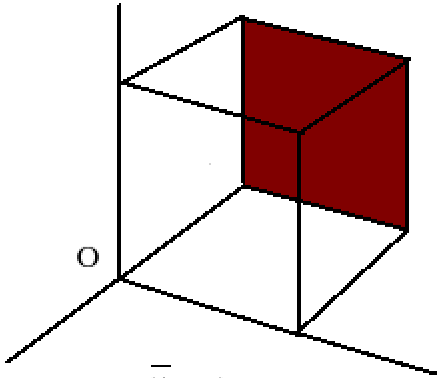

$(\bar{1}\ 0\ 0)$

Silicon (100)

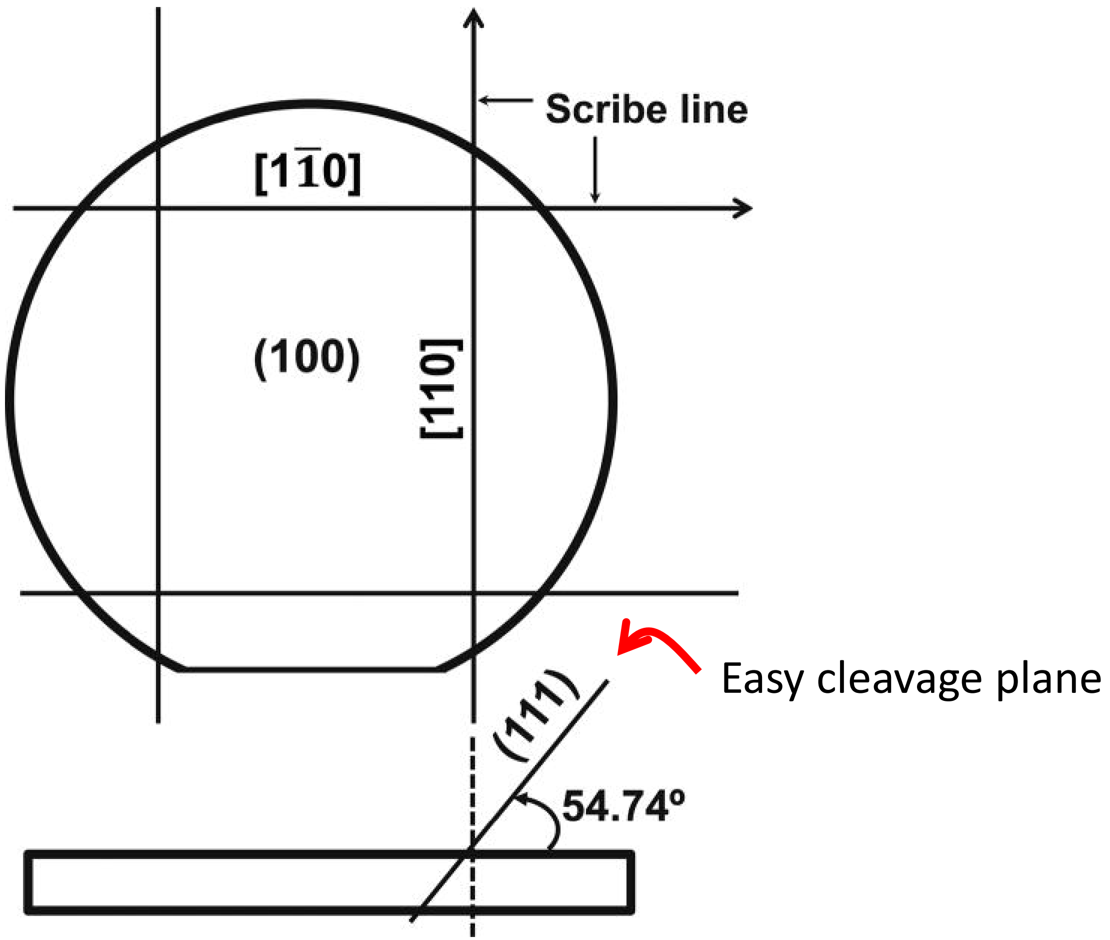

Silicon <100>

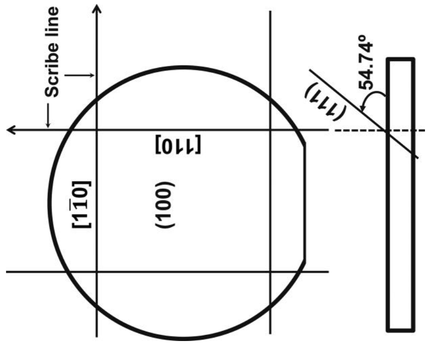

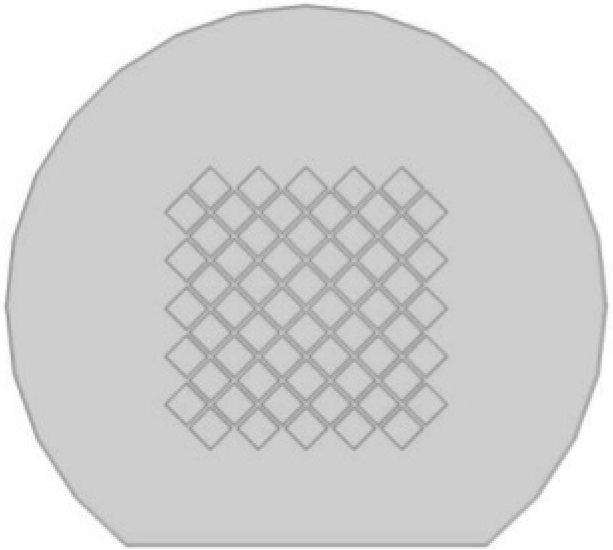

Top view

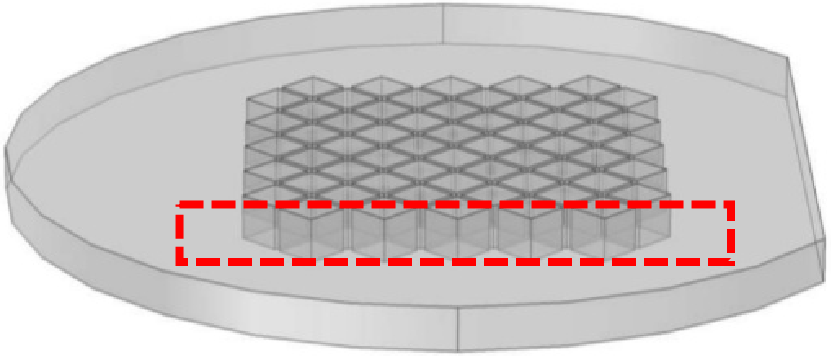

Side view

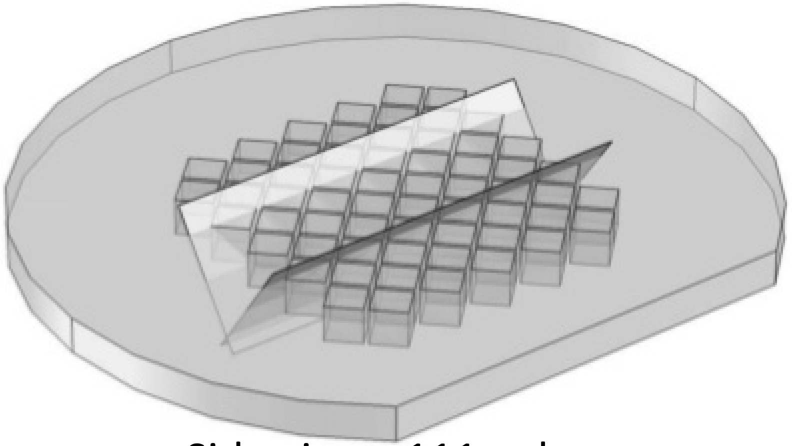

Side view <111> planes

View in <100> direction

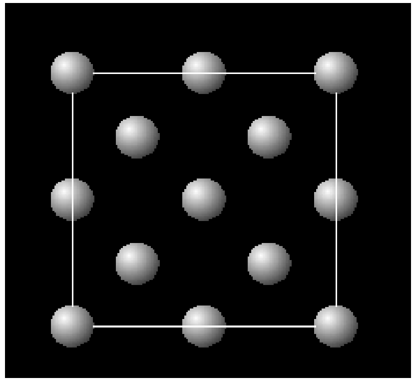

View in <110> direction

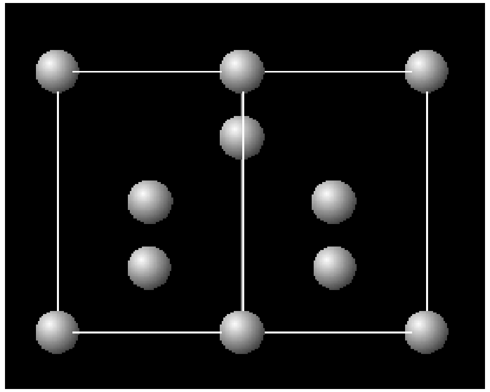

View in <111> direction

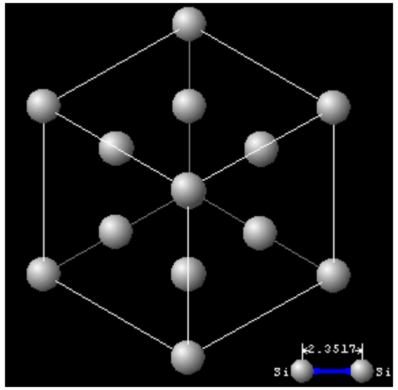

<111> planes of Silicon (cleaving planes)

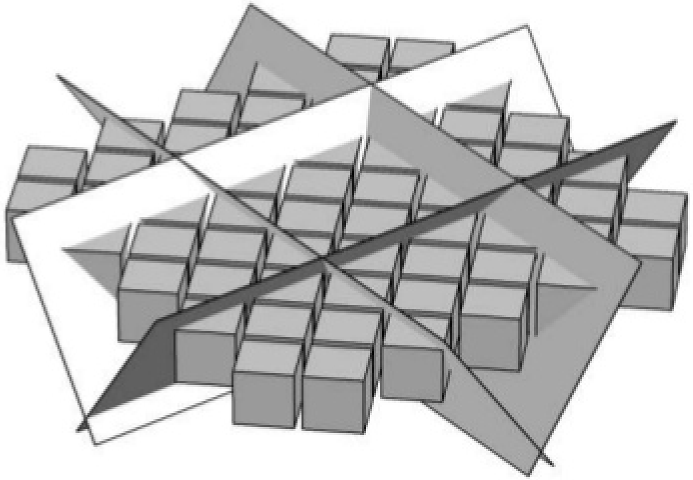

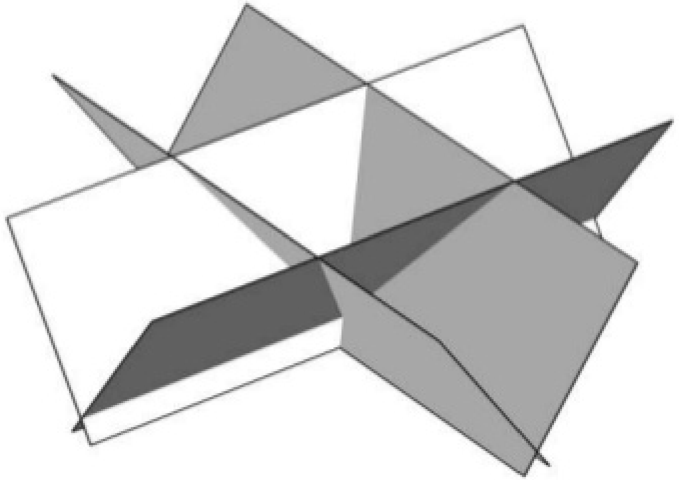

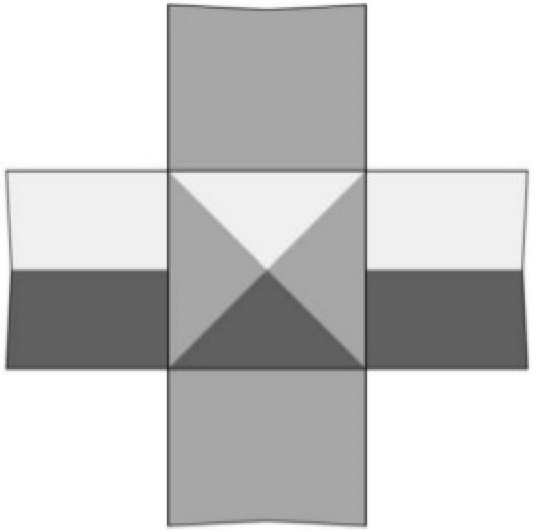

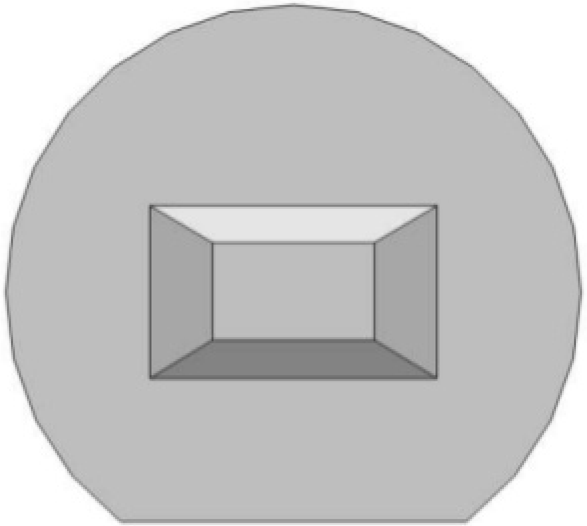

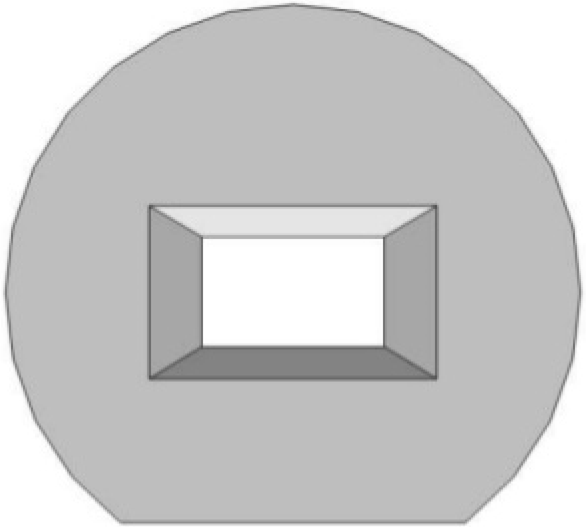

Drawings by Amid Adluy

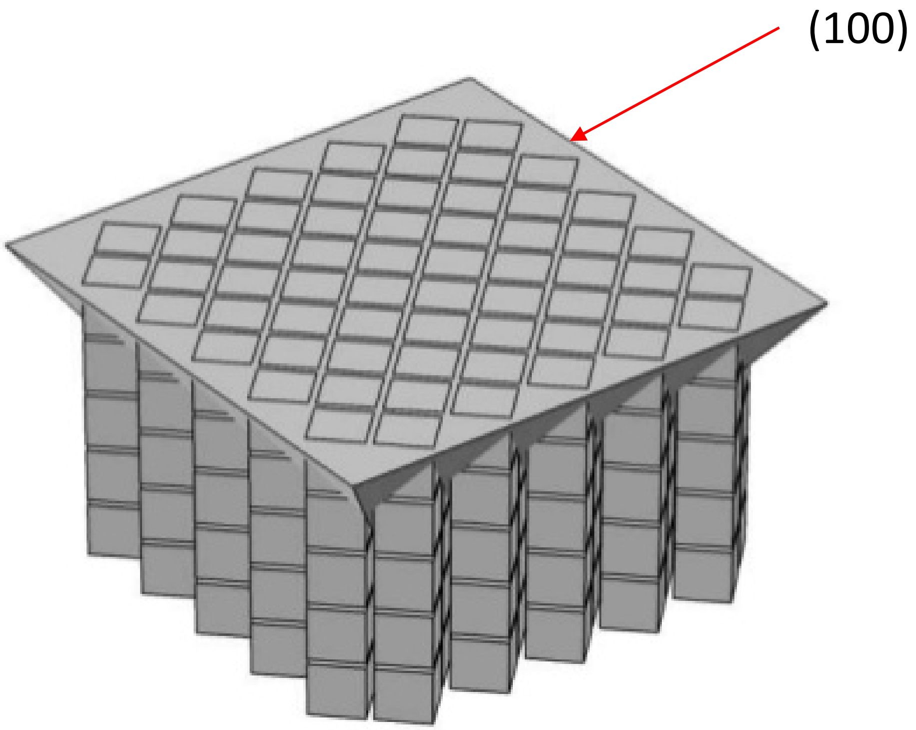

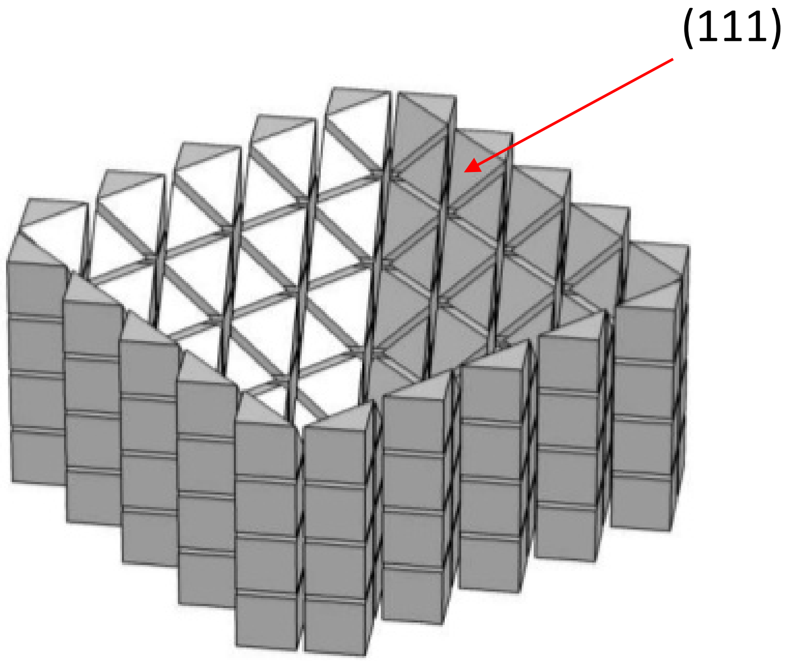

Drawings by Amid Adluy

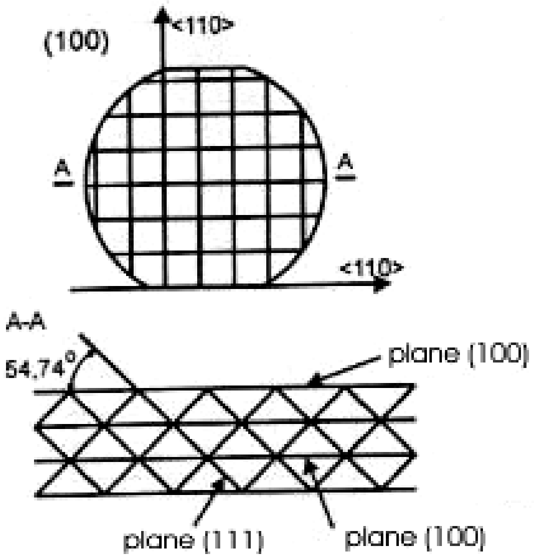
(100)
<110>
A
A
<110>
A-A
54,74°
plane (100)
plane (111)
plane (100)

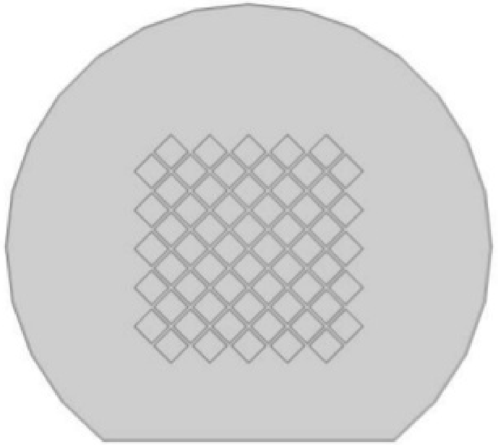

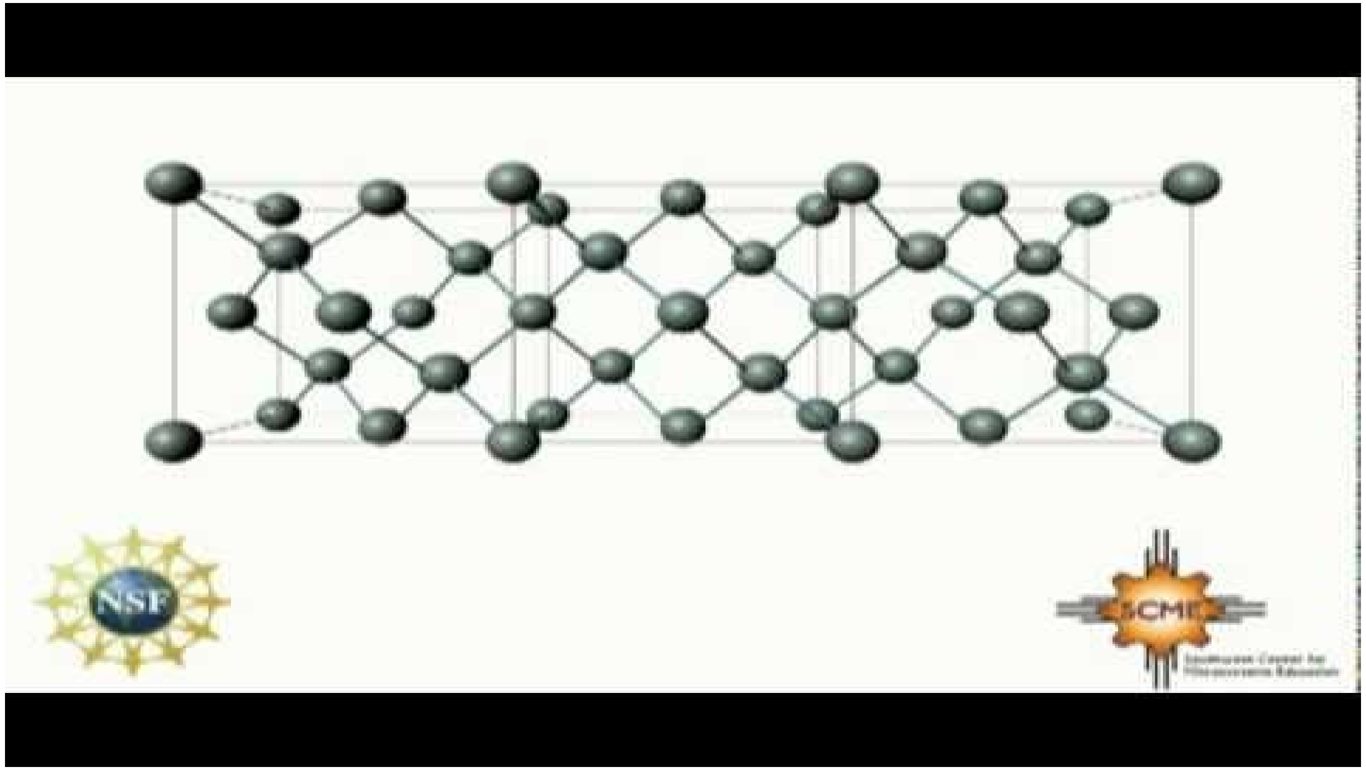

View in <100> direction

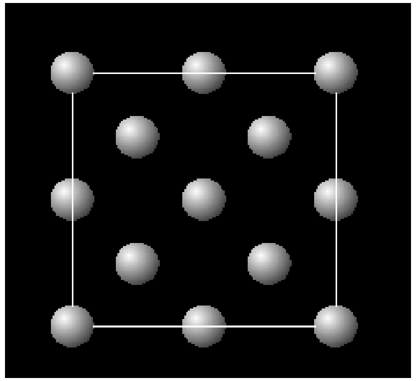

https://www.youtube.com/watch?v=XbBc4ByimY8

M. von Laue (1912)

Diffraction Grating

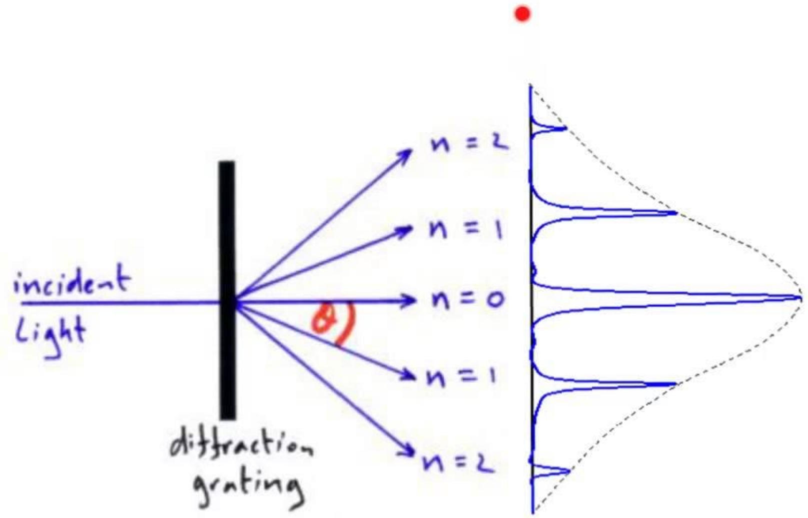

Light

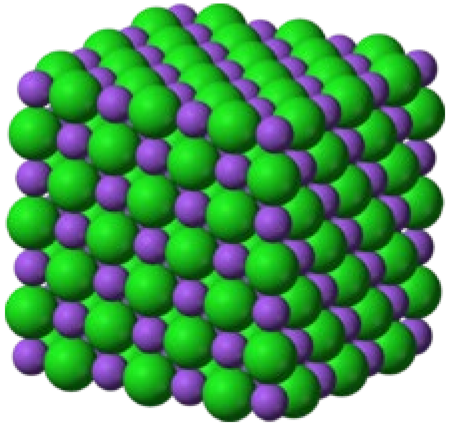

Diffraction
pattern
?

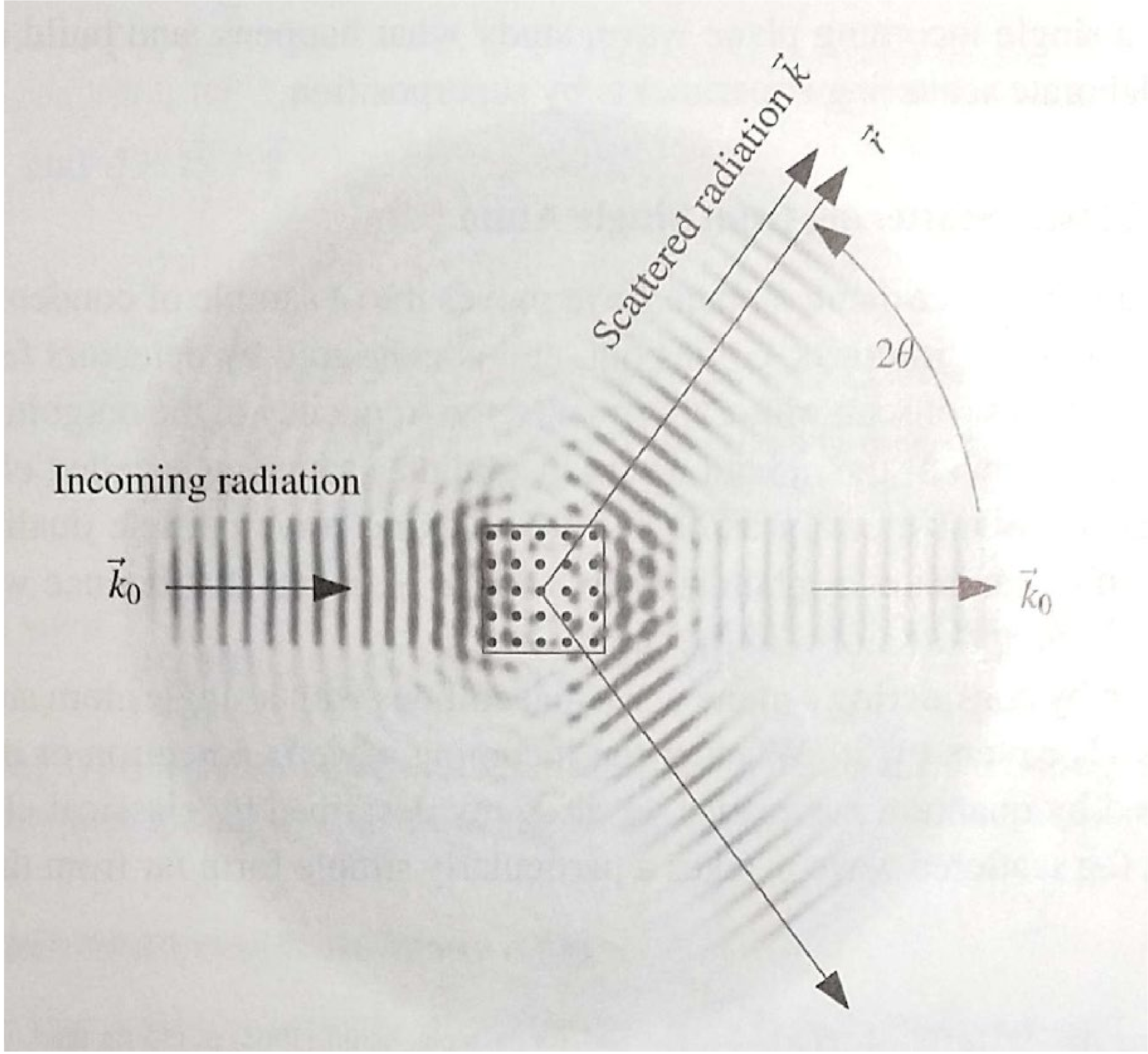

Scattered radiation $\vec{k}$
$\vec{r}$
2θ
Incoming radiation
$\vec{k}_0$
$\vec{k}_0$

First Brillouin zones

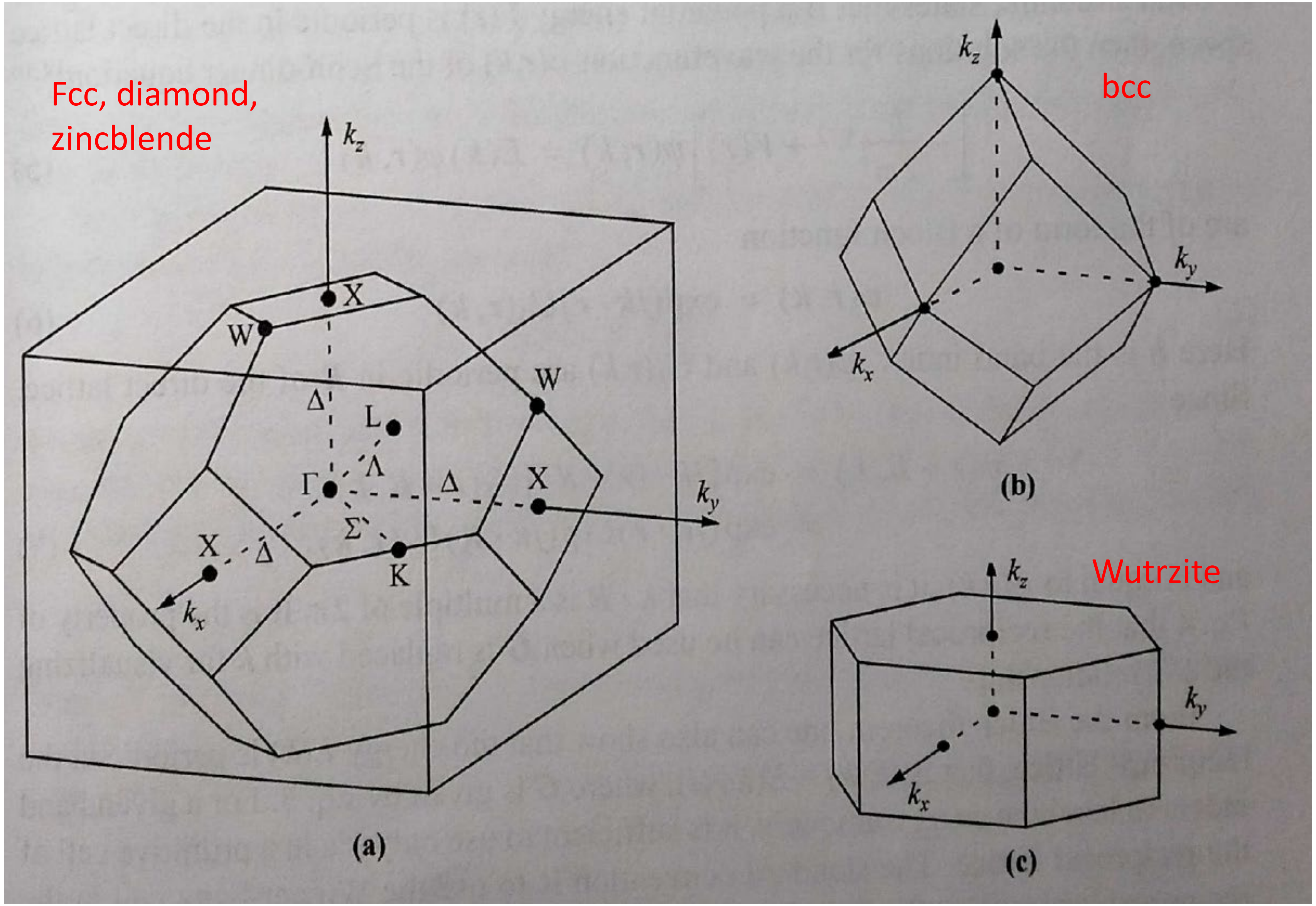

Reciprocal space basis vectors

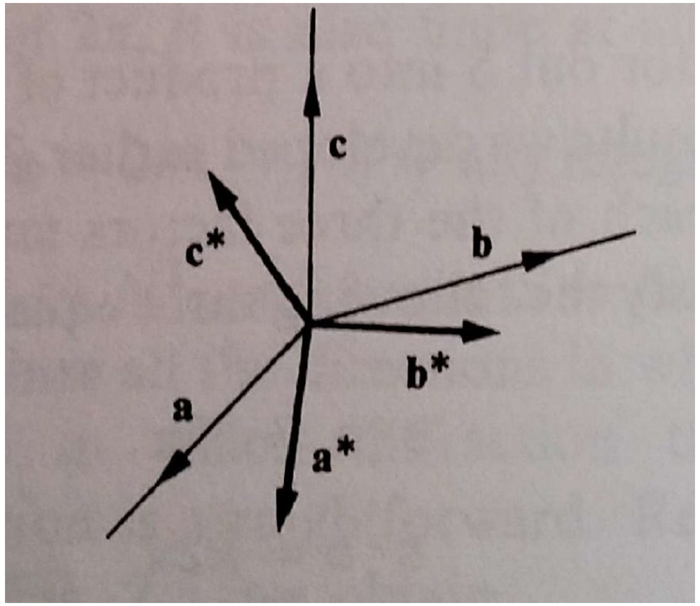

1D lattice

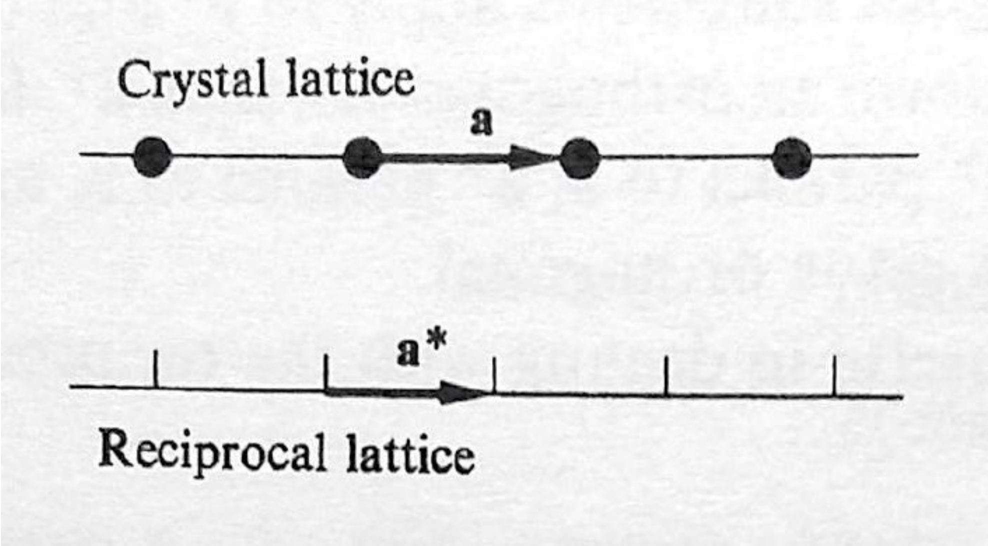

2D lattice

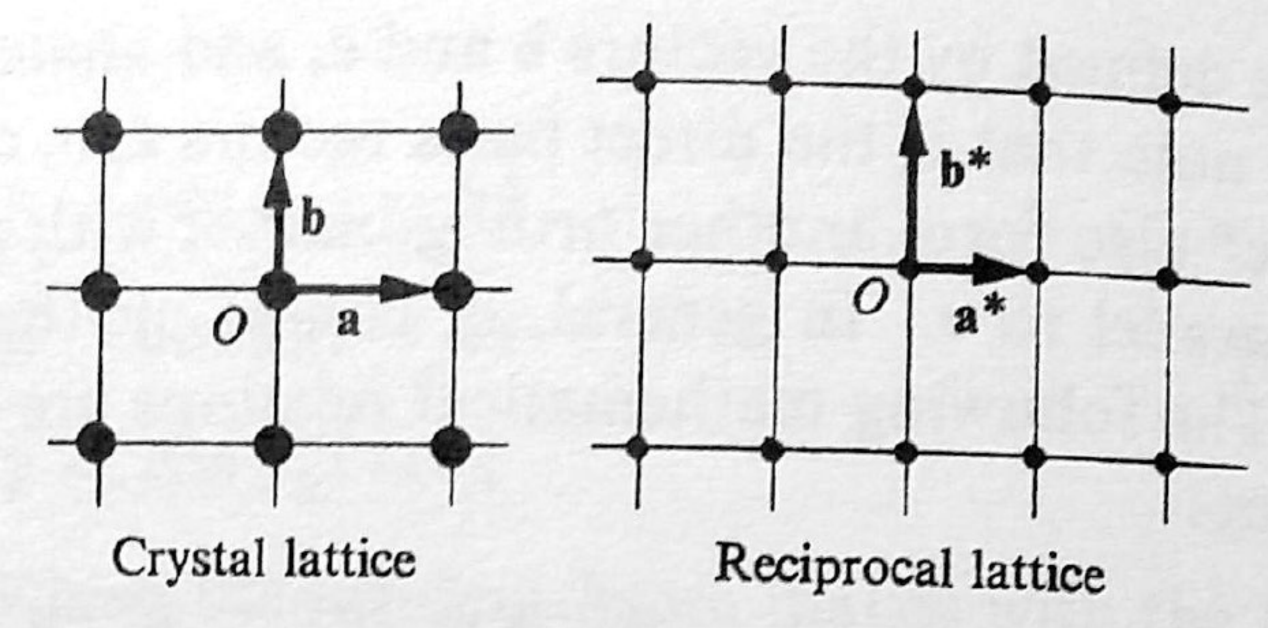

3D lattice

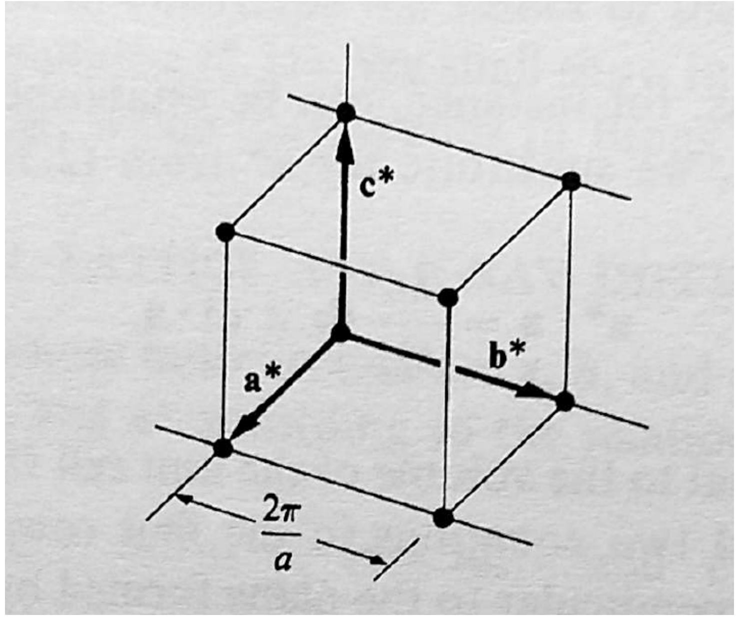

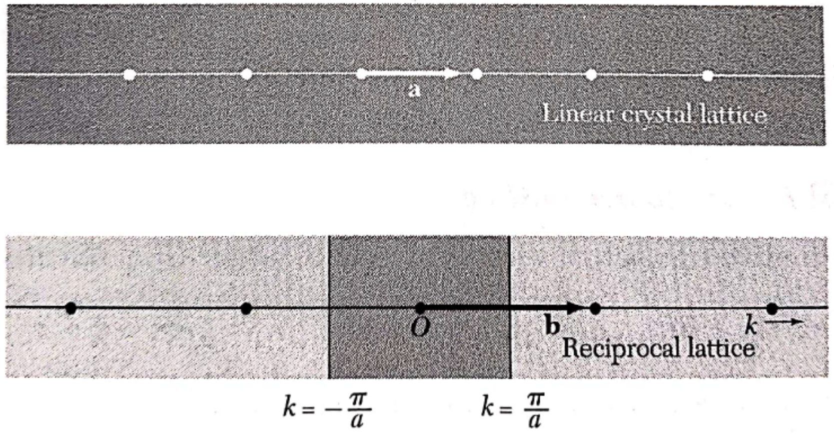

Figure 11 Crystal and reciprocal lattices in one dimension. The basis vector in the reciprocal lattice is **b**, of length equal to $2\pi/a$. The shortest reciprocal lattice vectors from the origin are **b** and $-$**b**. The perpendicular bisectors of these vectors form the boundaries of the first Brillouin zone. The boundaries are at $k = \pm\pi/a$.

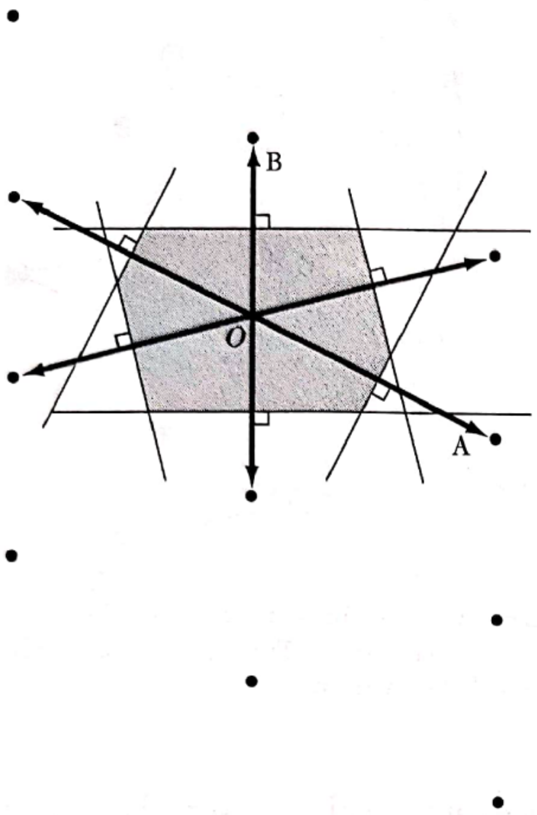

Figure 10 Construction of the first Brillouin zone for an oblique lattice in two dimensions. We first draw a number of vectors from O to nearby points in the reciprocal lattice. Next we construct lines perpendicular to these vectors at their midpoints. The smallest enclosed area is the first Brillouin zone.

Reciprocal space of a simple cubic (sc) lattice

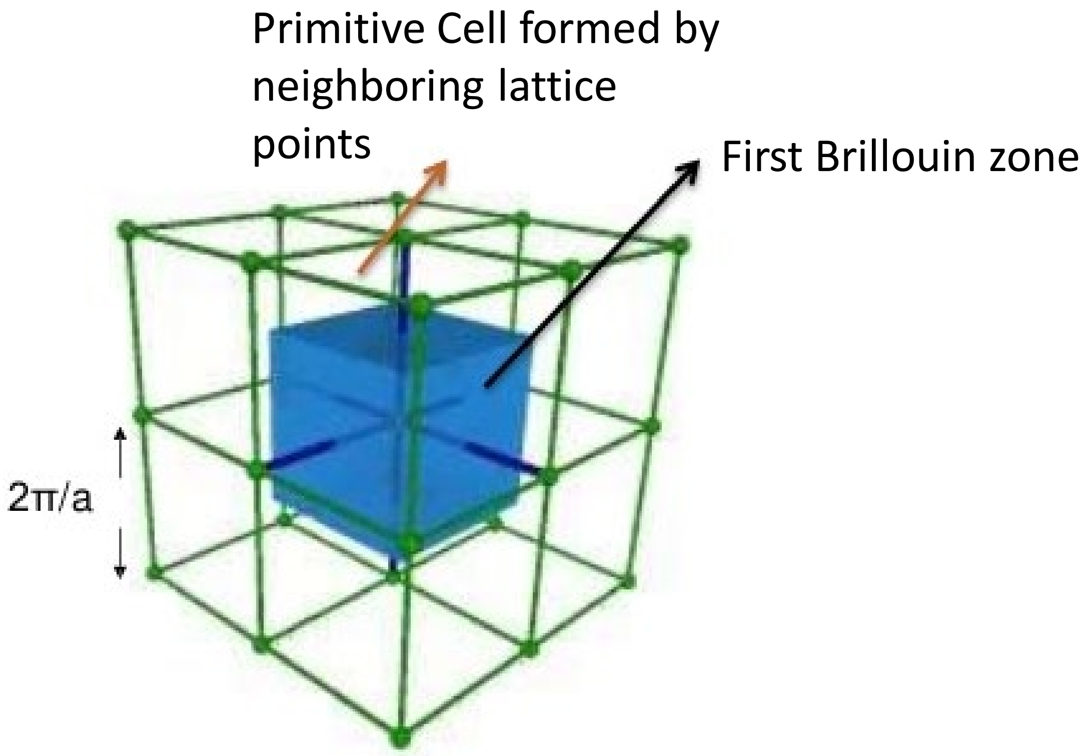

First Brillouin zone for fcc, diamond and zincblend → **Body centered cubic (bcc)**

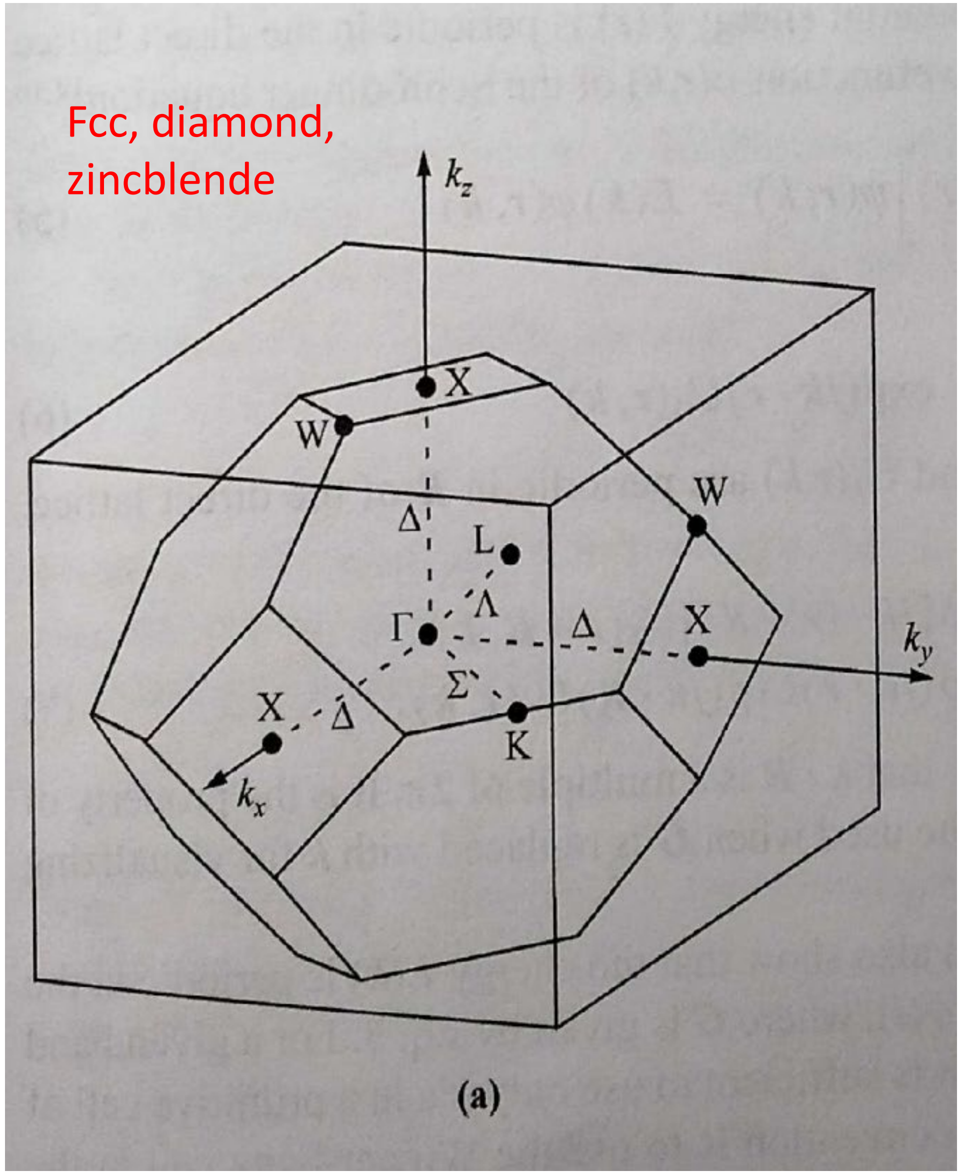

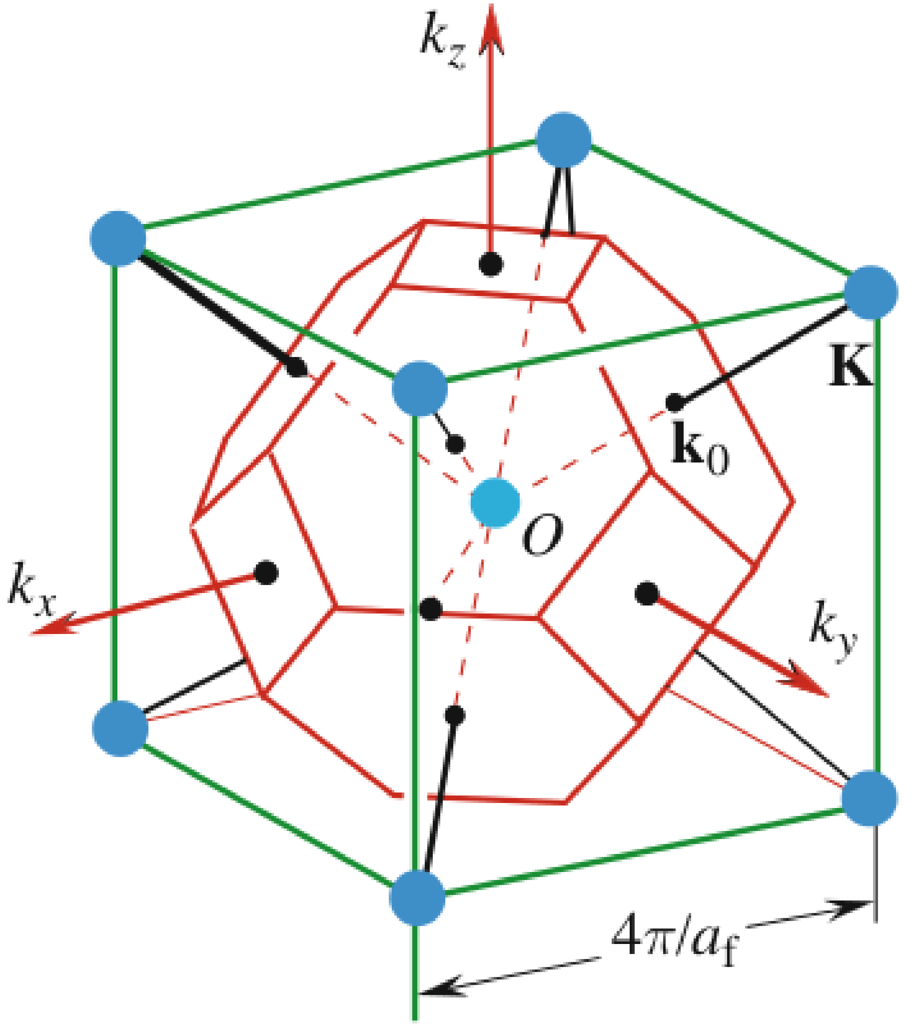

Face-centered cubic

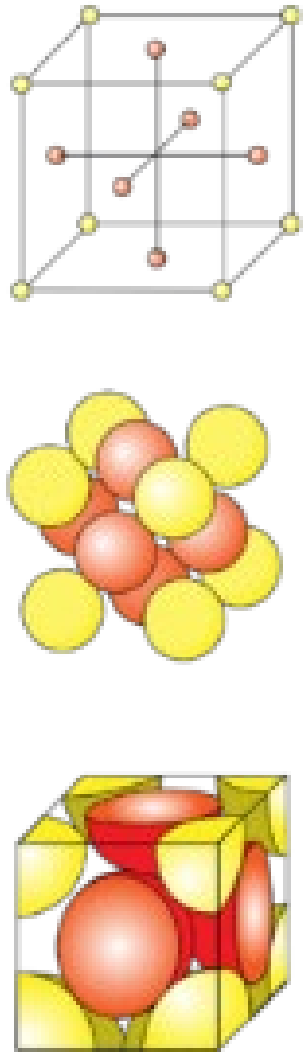

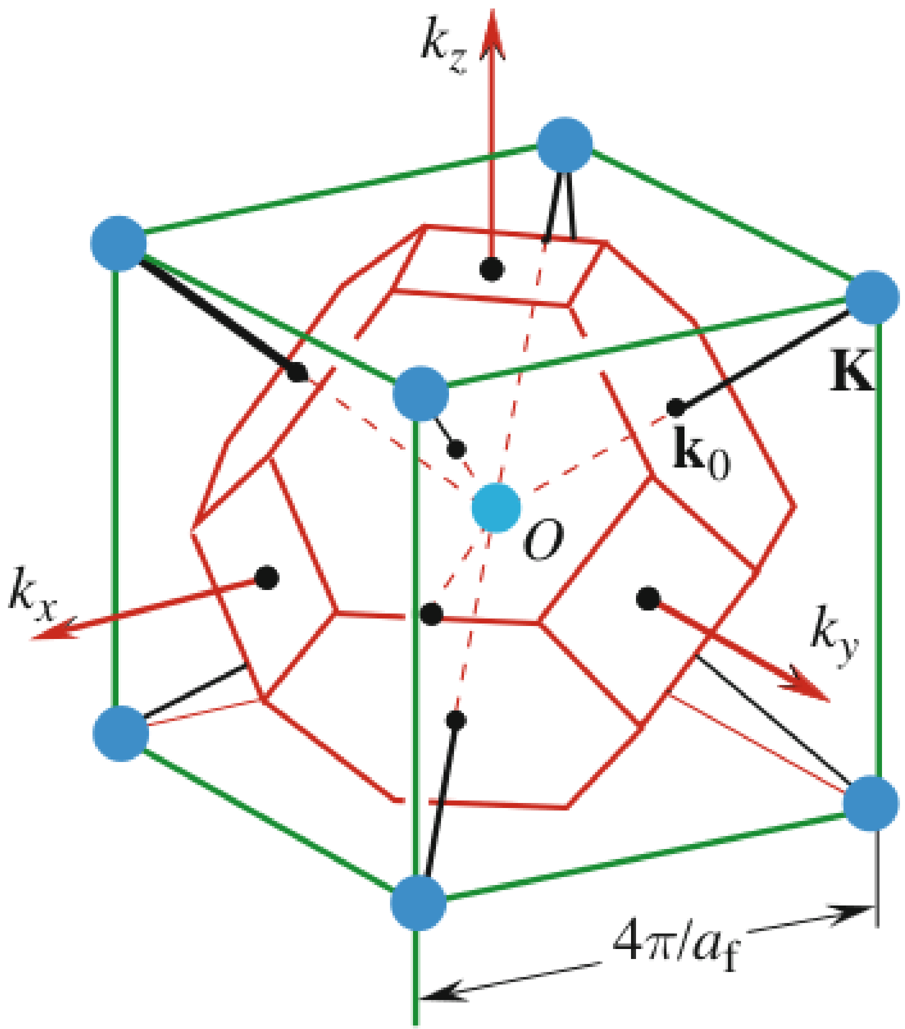

Band structure of Si and GaAs

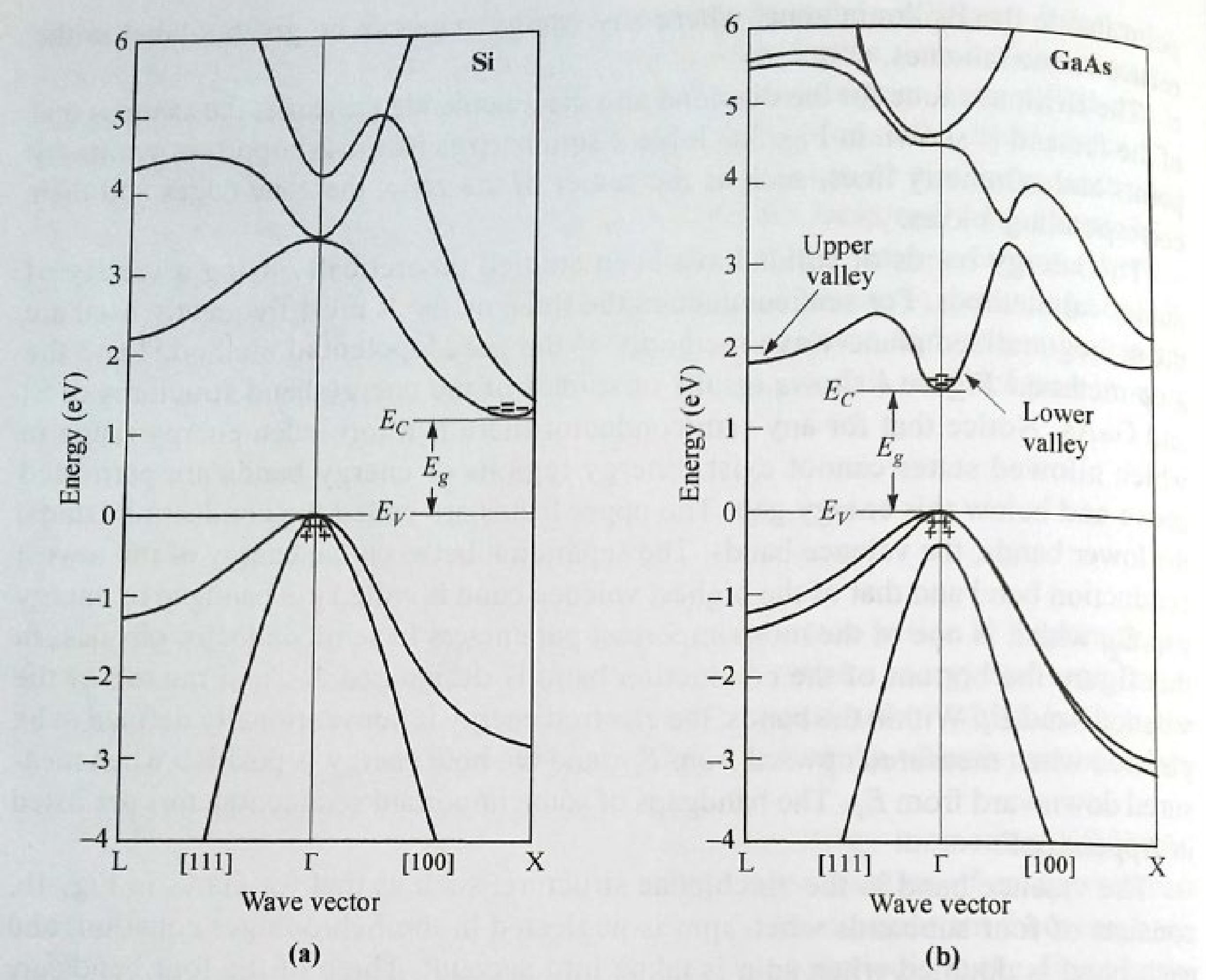

Fig. 4 Energy-band structures of (a) Si and (b) GaAs, where E_g is the energy bandgap. Plus signs (+) indicate holes in the valence bands and minus signs (–) indicate electrons in the conduction bands. (After Ref. 20.)

S. M. Sze and Kwok K. NG Physics of semiconductor devices

Properties of Important Semiconductors

	Semiconductor		Crystal Struct.	Lattice Const. at 300 K (Å)	Bandgap (eV)		Band	Mobility at 300 K (cm^2/V-s)		Effective Mass		$\varepsilon_s/\varepsilon_0$
					300 K	0 K		μ_n	μ_p	m_n^*/m_0	m_p^*/m_0	
	C	Carbon (diamond)	D	3.56683	5.47	5.48	I	1,800	1,200	0.2	0.25	5.7
	Ge	Germanium	D	5.64613	0.66	0.74	I	3,900	1,900	$1.64^l, 0.082^t$	$0.04^{lh}, 0.28^{hh}$	16.0
	Si	Silicon	D	5.43102	1.12	1.17	I	1,450	500	$0.98^l, 0.19^t$	$0.16^{lh}, 0.49^{hh}$	11.9
IV-IV	SiC	Silicon carbide	W	a=3.086, c=15.117	2.996	3.03	I	400	50	0.60	1.00	9.66
III-V	AlAs	Aluminum arsenide	Z	5.6605	2.36	2.23	I	180		0.11	0.22	10.1
	AlP	Aluminum phosphide	Z	5.4635	2.42	2.51	I	60	450	0.212	0.145	9.8
	AlSb	Aluminum antimonide	Z	6.1355	1.58	1.68	I	200	420	0.12	0.98	14.4
	BN	Boron nitride	Z	3.6157	6.4		I	200	500	0.26	0.36	7.1
	”	”	W	a=2.55, c=4.17	5.8		D			0.24	0.88	6.85
	BP	Boron phosphide	Z	4.5383	2.0		I	40	500	0.67	0.042	11
	GaAs	Gallium arsenide	Z	5.6533	1.42	1.52	D	8,000	400	0.063	$0.076^{lh}, 0.5^{hh}$	12.9
	GaN	Gallium nitride	W	a=3.189, c=5.182	3.44	3.50	D	400	10	0.27	0.8	10.4
	GaP	Gallium phosphide	Z	5.4512	2.26	2.34	I	110	75	0.82	0.60	11.1
	GaSb	Gallium antimonide	Z	6.0959	0.72	0.81	D	5,000	850	0.042	0.40	15.7
	InAs	Indium arsenide	Z	6.0584	0.36	0.42	D	33,000	460	0.023	0.40	15.1
	InP	Indium phosphide	Z	5.8686	1.35	1.42	D	4,600	150	0.077	0.64	12.6
	InSb	Indium antimonide	Z	6.4794	0.17	0.23	D	80,000	1,250	0.0145	0.40	16.8
II-VI	CdS	Cadmium sulfide	Z	5.825	2.5		D			0.14	0.51	5.4
	”	”	W	a=4.136, c=6.714	2.49		D	350	40	0.20	0.7	9.1
	CdSe	Cadmium selenide	Z	6.050	1.70	1.85	D	800		0.13	0.45	10.0
	CdTe	Cadmium telluride	Z	6.482	1.56		D	1,050	100			10.2
	ZnO	Zinc oxide	R	4.580	3.35	3.42	D	200	180	0.27		9.0
	ZnS	Zinc sulfide	Z	5.410	3.66	3.84	D	600		0.39	0.23	8.4
	”	”	W	a=3.822, c=6.26	3.78		D	280	800	0.287	0.49	9.6
IV-VI	PbS	Lead sulfide	R	5.9362	0.41	0.286	I	600	700	0.25	0.25	17.0
	PbTe	Lead telluride	R	6.4620	0.31	0.19	I	6,000	4,000	0.17	0.20	30.0

D = Diamond, W = Wurtzite, Z = Zincblende, R = Rock salt. I, D = Indirect, direct bandgap. l, t, lh, hh = Longitudinal, transverse, light-hole, heavy-hole effective mass.

Temperature dependence of the bandgap

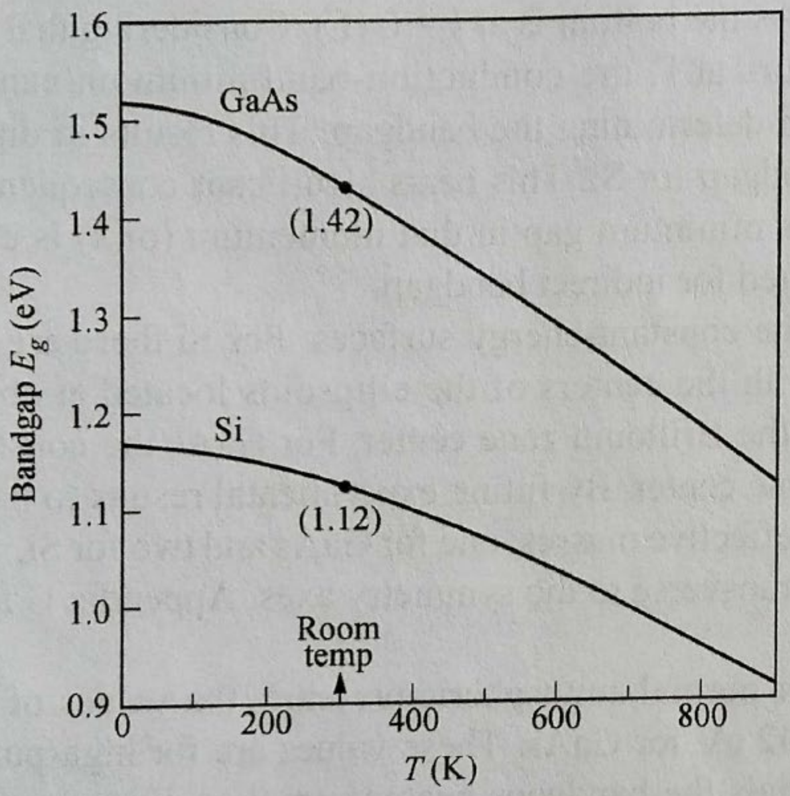

	$E_g(0)$ (eV)	α (eV/K)	β (K)
GaAs	1.519	5.4×10^{-4}	204
Si	1.169	4.9×10^{-4}	655

$$E_g(T) = E_g(0) - \frac{\alpha T^2}{T+\beta}$$

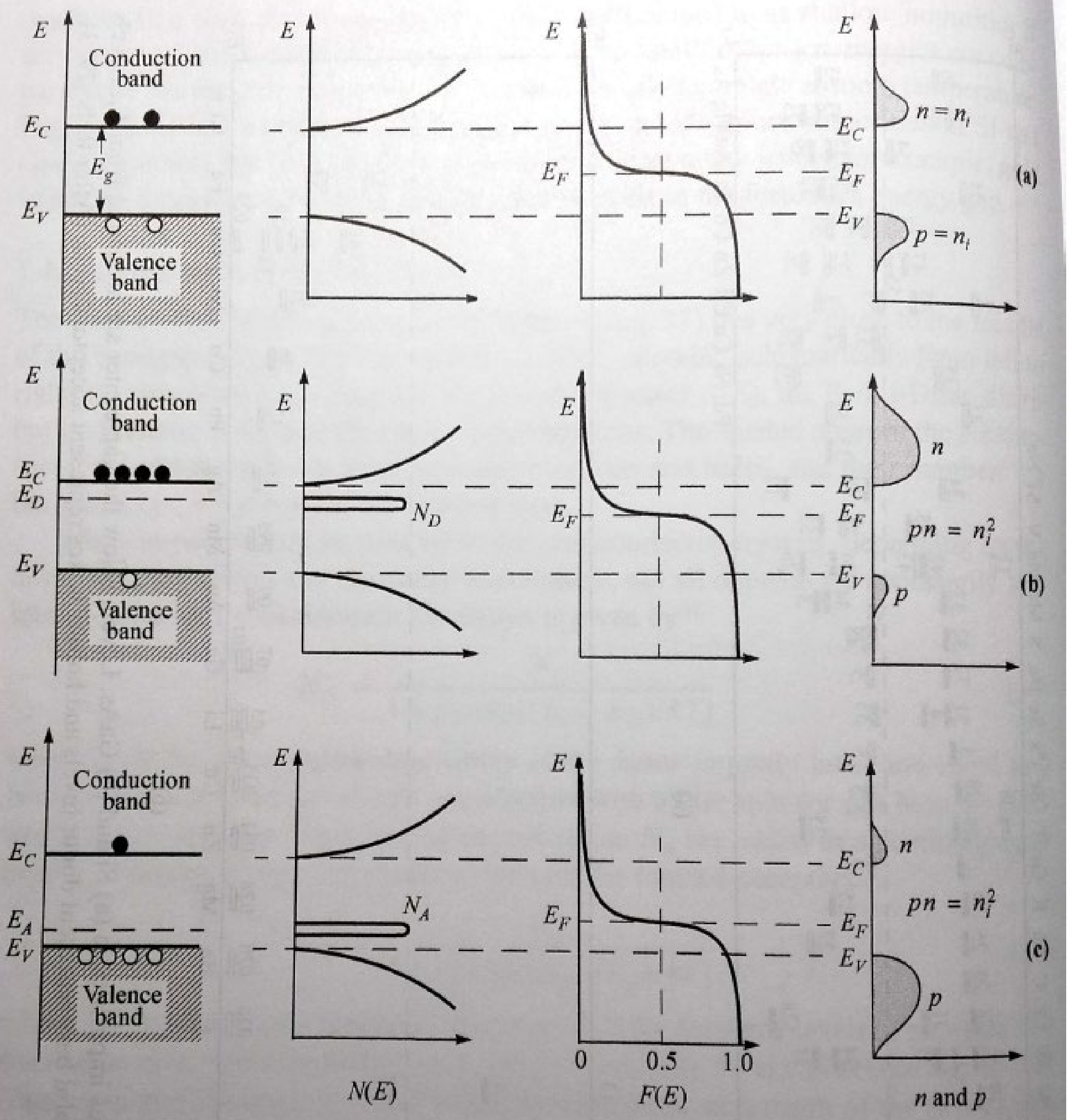

Fig. 11 Schematic band diagram, density of states, Fermi-Dirac distribution, and carrier concentrations for (a) intrinsic, (b) *n*-type, and (c) *p*-type semiconductors at thermal equilibrium. Note that $pn = n_i^2$ for all three cases.

Resistivity as a function of impurity concentration

Silicon

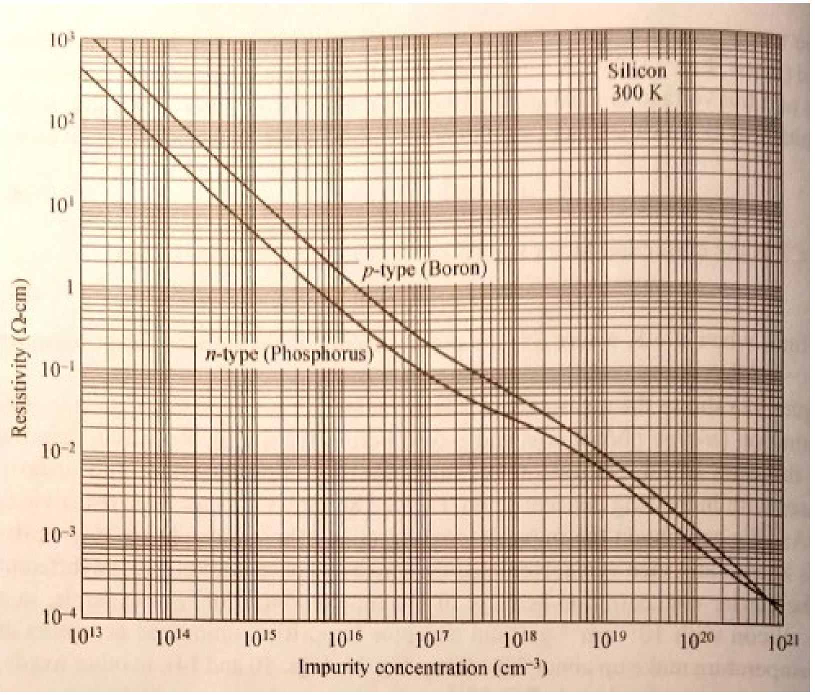

GaAs

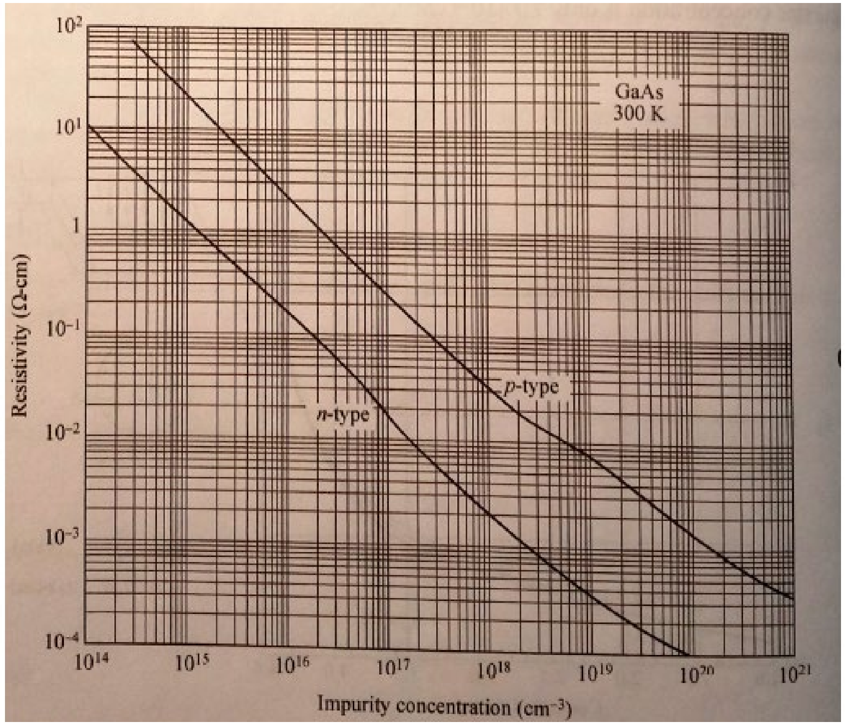

Sze, Physics of semiconductor devices

Band to band electron recombination

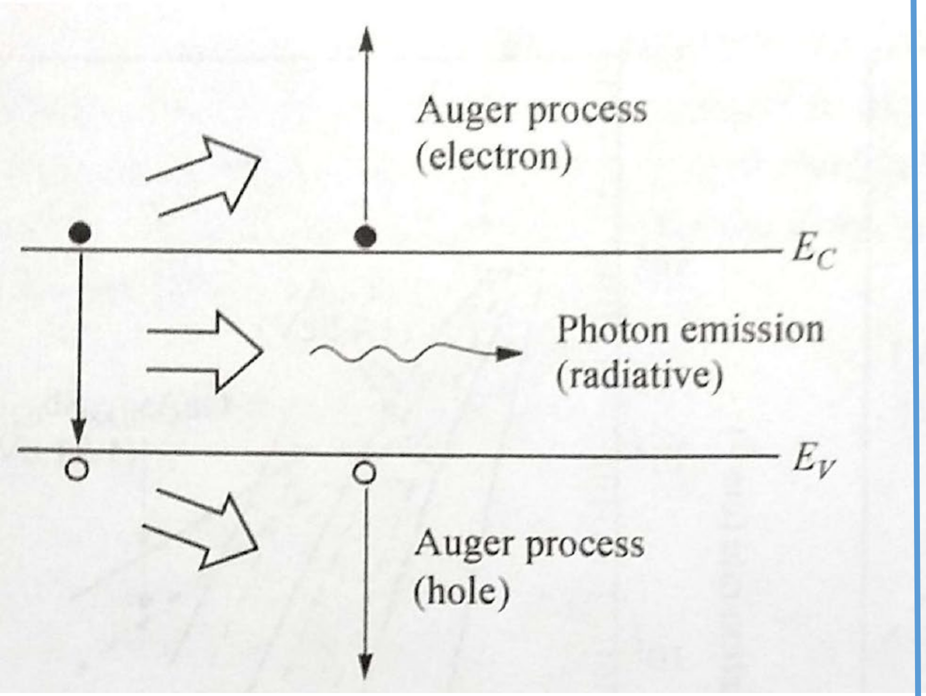

- Emission of a photon

Or

- Auger process

Recombination through single level traps

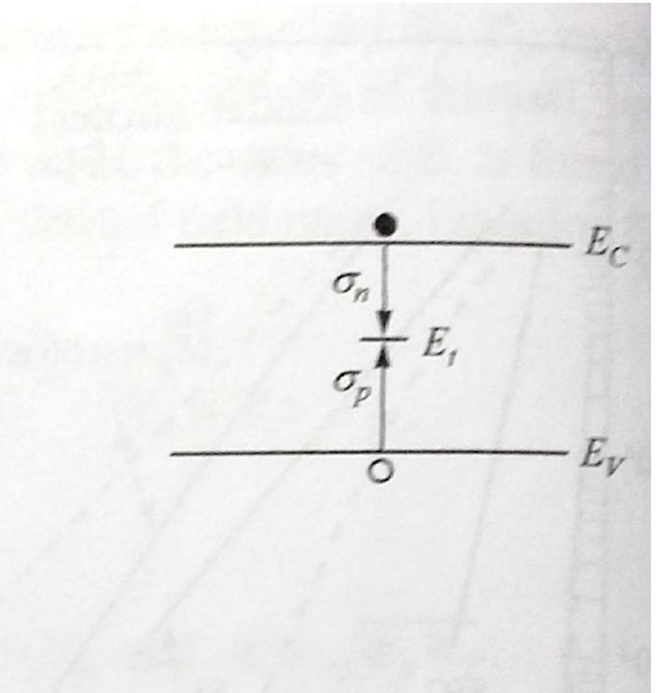

Energy and hole are captured in a trap inside the band gap

Recombination processes are relevant in the functioning of a solar cell

How does a solar cell work?

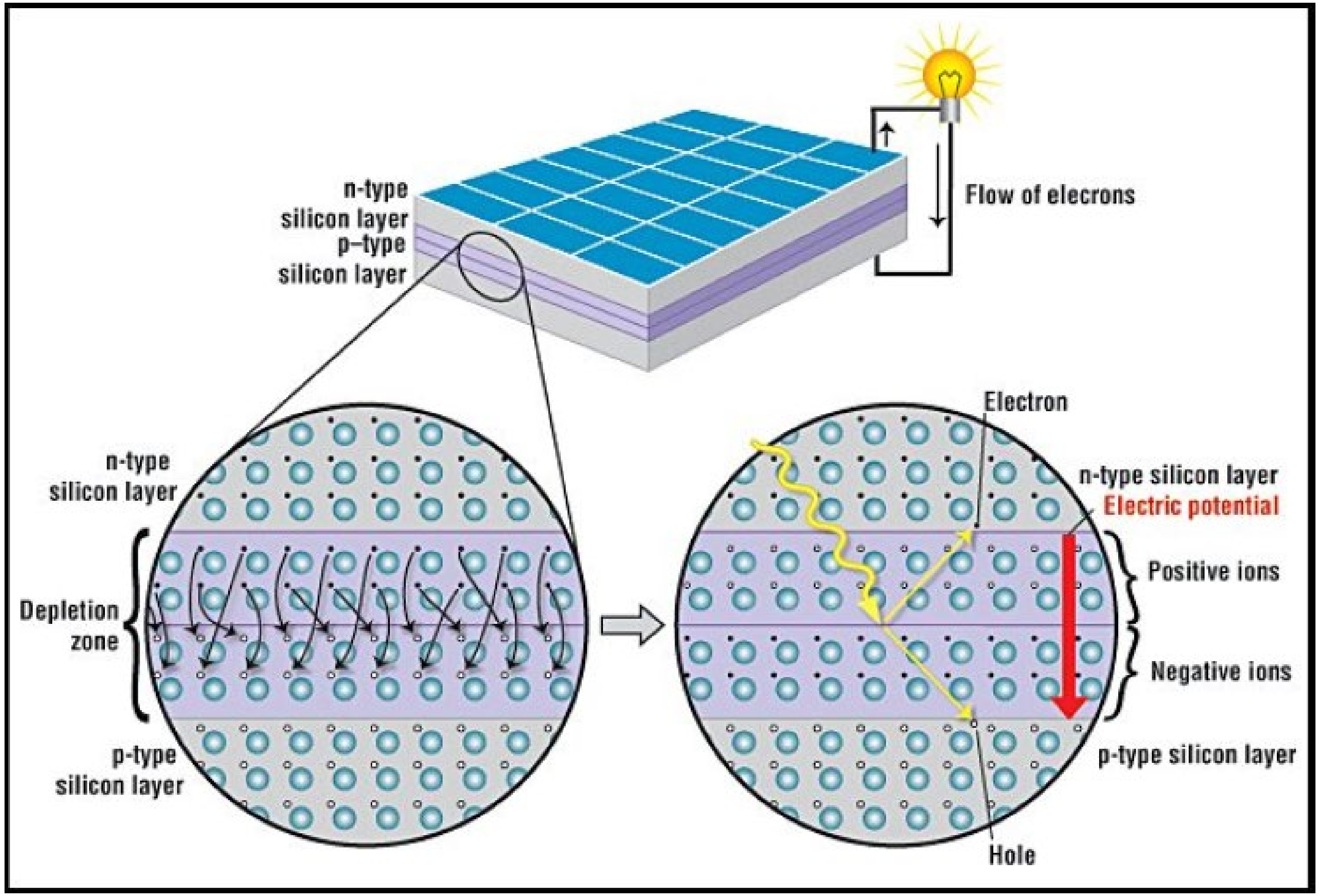

Energy band diagram showing thermionic emission of the electrons over the barrier

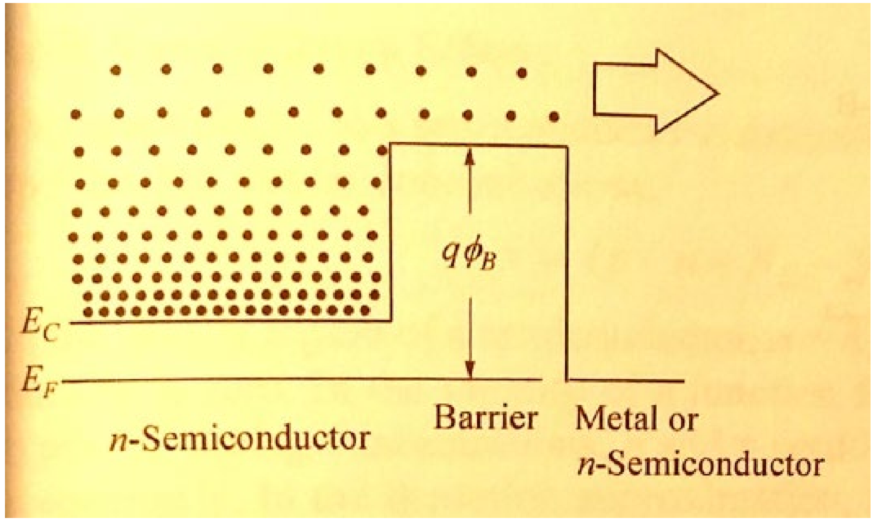

(The shape of the barrier does not matter)

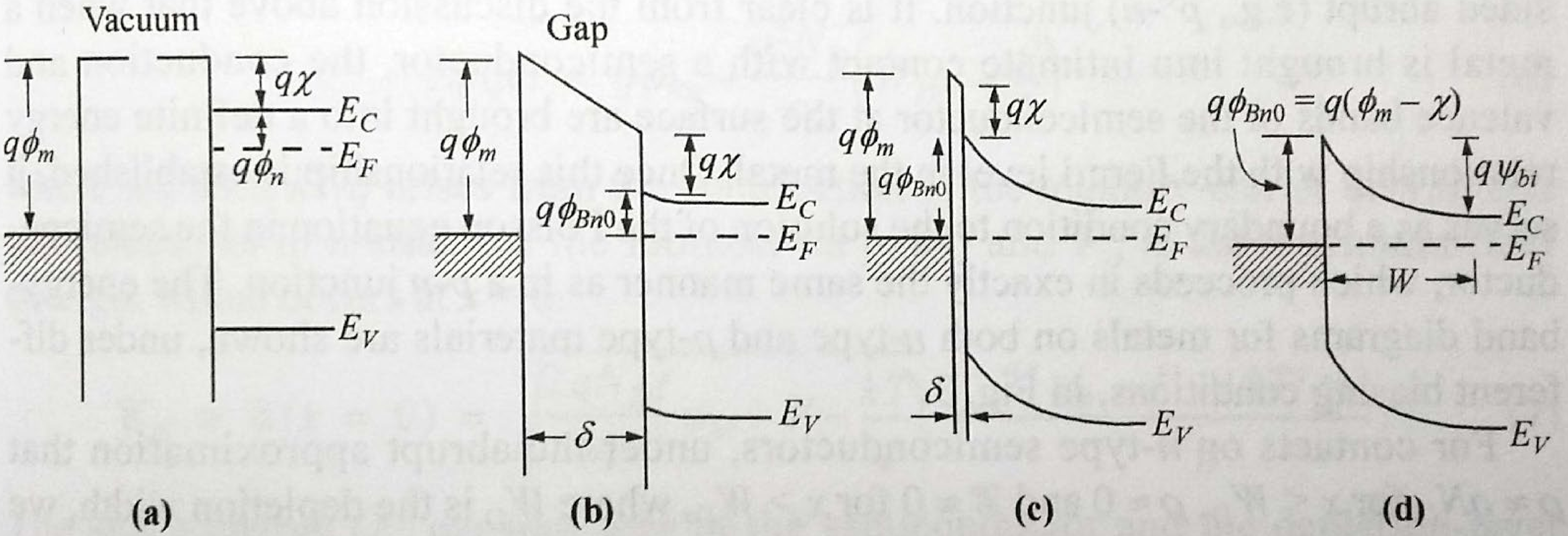

Fig. 1 Energy-band diagrams of metal-semiconductor contacts. Metal and semiconductor (a) in separated systems, and (b) connected into one system. As the gap δ (c) is reduced and (d) becomes zero. (After Ref. 7.)

APPLIED PHYSICS LETTERS **101**, 023102 (2012)

Towards spin injection from silicon into topological insulators: Schottky barrier between Si and Bi_2Se_3

C. Ojeda-Aristizabal, M. S. Fuhrer, N. P. Butch,[a)] J. Paglione, and I. Appelbaum
Center for Nanophysics and Advanced Materials, University of Maryland, College Park, Maryland 20742-4111, USA

(Received 23 May 2012; accepted 19 June 2012; published online 9 July 2012)

A scheme is proposed to electrically measure the spin-momentum coupling in the topological insulator surface state by injection of spin polarized electrons from silicon. As an initial approach, devices were fabricated consisting of thin (<100 nm) exfoliated crystals of Bi_2Se_3 on n-type silicon with independent electrical contacts to silicon and Bi_2Se_3. Analysis of the temperature dependence of thermionic emission in reverse bias indicates a barrier height of 0.34 eV at the Si-Bi_2Se_3 interface. This robust Schottky barrier opens the possibility of original device designs based on sub-band gap internal photoemission from Bi_2Se_3 into Si. [http://dx.doi.org/10.1063/1.4733388]

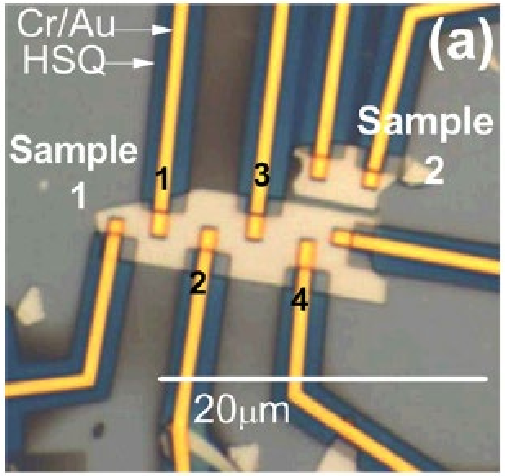

$$J = -A^*T^2 \exp\left(-\frac{q\phi_B}{k_B T}\right), \qquad (1)$$